

Recent Photoproduction Results From ZEUS

R. Saunders

for the ZEUS collaboration

University College London, Gower St., London, WC1E 6BT, England

Abstract. Recent results for inclusive jet cross sections, dijet cross sections and dijet angular distributions are compared with NLO perturbative QCD calculations. The observation of isolated high P_T photons (prompt photons) is also reported.

INTRODUCTION

Collisions of 27.5 GeV positrons with 820 GeV protons at **HERA** are studied using the **ZEUS** detector. The processes of interest here are those where an almost real photon (virtually $P^2 \approx 0$) is radiated from the positron which then interacts with a parton in the proton to produce two high transverse energy jets. The hard scale provided by the large transverse momentum allows us to describe these processes using perturbative QCD (pQCD), and therefore they can be used to test it. The photon can either interact directly with the parton from the proton (direct processes), or it can first fluctuate into an hadronic state which then acts as source of partons for the hard scatter (resolved processes). In the resolved case, in addition to the two jets, there is also a photon remnant. In direct process since all the photon takes part in the interaction x_γ , the fraction of the photon momentum entering into the hard scatter, is 1, and conversely for resolved processes $x_\gamma < 1$. In order to use this to identify and separate direct and resolved event samples it is necessary to define an experimentally measurable x_γ that is valid to all orders. This is done in terms of the transverse energy E_t^{jet} and pseudorapidity $\eta^{jet} = -\ln(\tan \frac{\theta^{jet}}{2})$ of the two highest transverse energy jets in an event [1]:

$$x_\gamma^{OBS} = \frac{1}{2yE_e} \left(E_t^{jet1} e^{-\eta^{jet1}} + E_t^{jet2} e^{-\eta^{jet2}} \right) \quad (1)$$

Higher order and hadronisation effects cause the average x_γ^{OBS} of direct events to be slightly less than 1, and the distribution peaks at ~ 0.85 . A cut at

ZEUS 94 Preliminary

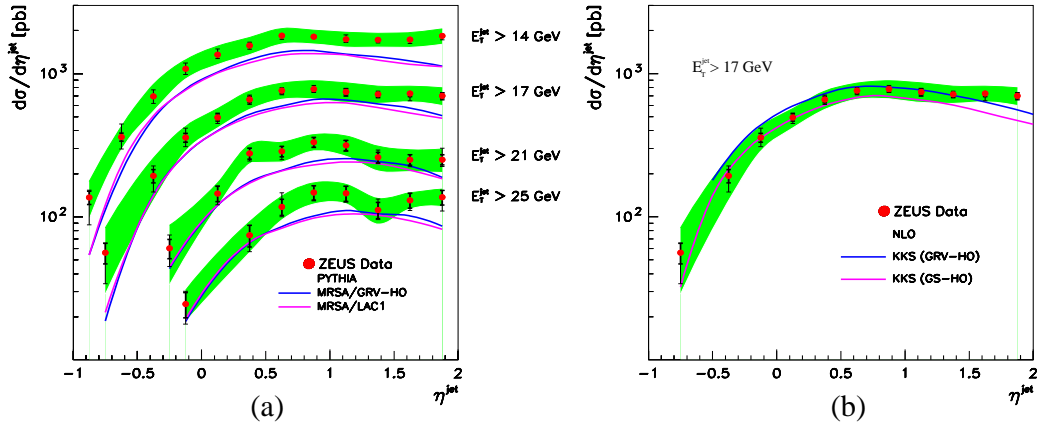


FIGURE 1. Inclusive jet cross sections. Thick error bars: statistical, thin error bars: systematic, shaded band: uncertainty due to the calorimeter energy scale.

$x_\gamma^{OBS} = 0.75$ is used to separate the two classes of event. Direct processes are sensitive to high x_γ quarks in the photon, and the parton distribution of the proton, whereas resolved process are sensitive to lower x_γ parton distributions in the photon. The results presented here are based on 2.7pb^{-1} of data taken in the 1994 HERA running period, except the prompt photon analysis which uses data corresponding to 5.7pb^{-1} from 1995. All cross sections presented here are corrected back to final state particle level using Monte Carlo.

INCLUSIVE JET CROSS SECTIONS

The cross section of the hard scatter is factorised into three parts: the parton-parton scattering cross section $\hat{\sigma}(ab \rightarrow j_1 j_2)$, the parton densities in the proton $f_{a/p}(x_p, Q^2)$, and those of the photon $f_{a/\gamma}(x_\gamma, Q^2)$. The jet cross section at leading order is written as

$$\frac{d\sigma(\gamma p \rightarrow j_1 j_2 X)}{dp_t^2 d\eta_1 d\eta_2} = \sum_a \sum_b x_p x_\gamma f_{a/p}(x_p, Q^2) \times f_{b/\gamma}(x_\gamma, Q^2) \frac{d\hat{\sigma}(ab \rightarrow j_1 j_2 X)}{d\hat{t}} \quad (2)$$

where η_1 and η_2 denote the pseudorapidities of the two outgoing partons. So by measuring jet cross sections one can test pQCD and gain insight into the parton densities in the proton and photon. At HERA we are looking at e-p collisions and there is a spectrum of incoming photon energies, usually described using the Weizsäcker-Williams approximation [6]. Here the inclusive jet cross section $\frac{d\sigma}{d\eta^{jet}}$ is presented for cone jets with a radius $R=1$ in $\eta - \phi$ space, with pseudorapidities $-1 < \eta^{jet} < 2$, in events with centre of mass

energies $134 < W = \sqrt{yE_e E_p} < 277$ GeV. The measurement is made for cuts on the minimum E_t^{jet} of 14, 17, 21, and 25 GeV. Figure 1(a) shows these cross sections compared to expectations from the PYTHIA model. PYTHIA simulates the matrix element in LO with the inclusion of initial and final state parton showers (PS). The shape of the cross sections is well described by the model, however the PYTHIA result is $\sim 30\%$ lower than the data in all cases. This is true for both GRV-HO and LAC1 parameterisations of the photon structure function. Figure 1(b) shows the curve for $E_t^{jet} > 17$ GeV compared to next to leading order (NLO) QCD calculations by Kramer, Klasen, and Salesch [2], using GRV-HO and GS parton distributions for the photon. The calculated and measured cross sections agree well in magnitude up to $\eta^{jet} \approx 1.3$ for both photon parton distribution functions. At larger rapidities the calculations tend to fall below the data.

DIJET CROSS SECTIONS

The dijet cross sections as a function of $\bar{\eta} = \frac{1}{2}(\eta^{jet1} + \eta^{jet2})$ have been measured in order to study the photon and proton structure. The requirement $|\eta^{jet1} - \eta^{jet2}| < 0.5$ is made to increase correlation to the parton momenta and ensure a good resolution for the measurement. The measurement was made with a clustering algorithm KTCLUS [3], and two types of cone algorithm EUCELL and PUCCELL (both with a cone radius of 1). These algorithms differ in their seed finding and cone merging. Figure 2(a) shows the measured cross sections for all three jet finders for minimum E_t^{jet} cuts of 6, 8, 11, and 15 GeV. The upper four plots are for $x_\gamma^{OBS} > 0.75$, and the lower four for $0.3 < x_\gamma^{OBS} < 0.75$. To model the differences in the jet algorithms in NLO calculations an additional parameter, R_{sep} , is introduced [4,5]. Curves for $R_{sep} = 1$ and $R_{sep} = 2$ are also shown in figure 2(a). $R_{sep} = 1$ emulates KTCLUS and $R_{sep} = 1R$ ($\approx 1.5 - 2R$) PUCCELL (EUCELL). At lower E_t^{jet} the differences between the two calculations and the different jet algorithms are similar. As the E_t^{jet} rises the differences between the measurements gradually disappear, however the differences between the calculations remain. For the high x_γ^{OBS} cross sections there is good agreement between the measurements and the respective calculation. The same is true for the low x_γ^{OBS} results with $E_t^{jet} > 11$ GeV. However, when lower energy jets are included the data lie significantly above the calculations.

DIJET ANGULAR DISTRIBUTIONS

In it's CMS the dijet system is characterised by a scattering angle θ^* , the angle between the jets and the beam axis. The dominant direct photon process is photon-gluon fusion ($\gamma g \rightarrow q\bar{q}$) where the exchanged particle is a quark. This

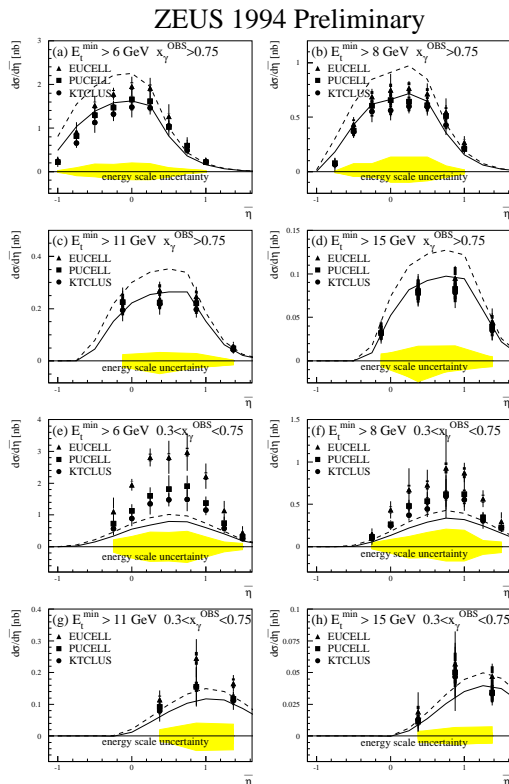


FIGURE 2. Dijet cross sections. Points: data using different jet algorithms, thin (thick) error bars: systematic (statistical), shaded band: calorimeter energy scale uncertainty. The curves are NLO calculations with $R_{sep} = 1$ (solid) and $R_{sep} = 2$ (dashed).

fermion exchange leads to a $(1 - |\cos\theta^*|)^{-1}$ angular dependence in the cross section. In contrast resolved processes are dominated by gluon exchange, which results in an angular dependence of $(1 - |\cos\theta^*|)^{-2}$. Therefore low and high x_γ^{OBS} samples should have different angular distributions. Figure 3(a) shows the measured $\frac{d\sigma}{d|\cos\theta^*|}$ for direct and resolved event samples normalised to unity at $|\cos\theta^*| = 0$. Also shown are curves for LO and NLO calculations [7]. As expected, the resolved sample shows a much steeper rise towards high $|\cos\theta^*|$ than the direct sample. The data and calculations are in excellent agreement. This confirms that direct (resolved) photoproduction is dominated by the exchange of spin- $\frac{1}{2}$ quarks (spin-1 gluons).

PROMPT PHOTON

The dominant prompt photon processes are $qg \rightarrow \gamma q$ and $q\bar{q} \rightarrow \gamma g$ for resolved, and $\gamma q \rightarrow q\gamma$ for direct photoproduction. Therefore prompt photon measurements are particularly sensitive to the quark distributions in the proton and photon. Direct processes are expected to dominate overall. The

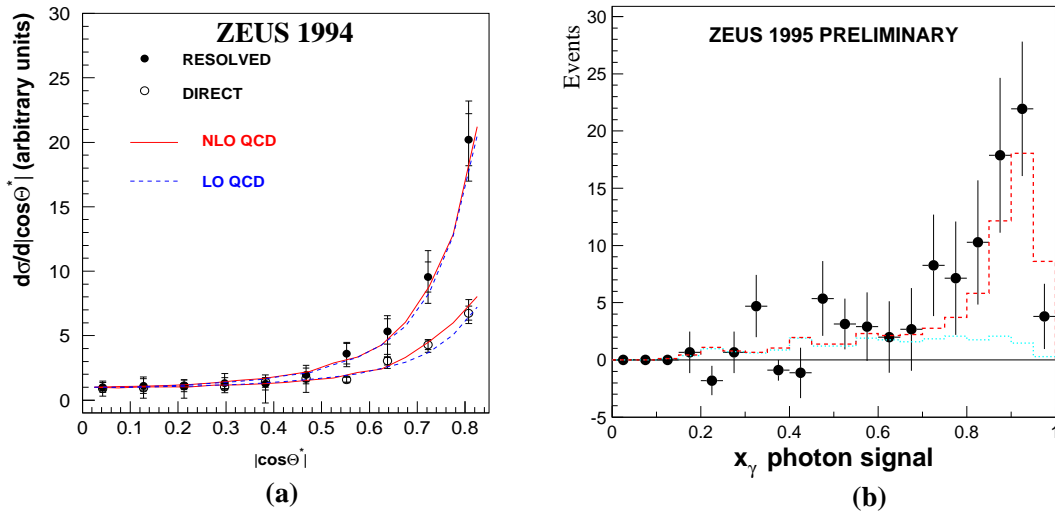


FIGURE 3. (a) Dijet angular distributions Compared to LO and NLO calculations. (b) Observed x_γ distribution for prompt photon events compared to direct+resolved (Dashed line), and resolved only (Dotted line) PYTHIA samples.

advantage of the photon in the final state over jets is that it is not subject to hadronisation effects. Events are selected if they contain at least one jet with $E_t > 4$ GeV and one prompt photon. The photons are identified as an electromagnetic cluster in the calorimeter with $5 < E_T < 10$ GeV and no track within a radius of 0.3 in $\eta - \phi$ space. Figure 3(b) shows as points the measured x_γ distribution for these events. Also shown are histograms for full, and resolved only PYTHIA Monte Carlo samples. This plot confirms that the direct processes dominate.

REFERENCES

1. ZEUS Collaboration, *Phys. Lett.* **B 348**, 665-680 (1995).
2. M. Klasen, G. Kramer and S. G. Salesch, *Z. Phys.* **C 68**, 113 (1995).
3. S. Catani, Yu.L. Dokshitzer, M.H. Seymour and B.R. Webber, *Nucl. Phys.* **B 406** 187 (1993).
4. S.D. Ellis, Z. Kunszt, D.E. Soper, *Phys. Rev. Lett.* **69** 3615 (1992).
5. J. M. Butterworth, L. Feld, M. Klasen and G. Kramer, hep-ph 9608481; *Proceedings of the workshop Future Physics at HERA* 554 (1996).
6. C.F.v. Weizsäcker, *Z. Phys.* **bf 88**, 612 (1934)
E. J. Williams, *Phys. Rev.*, **45**, 729 (1934).
7. H. Baer, J. Ohnemus and J.F. Owens *Phys. Rev.* **D 40**, 2844 (1989);
J.F. Owens, private communication.
8. M. Klasen, G. Kramer DESY-96-246, hep-ph/9611450.